

$B_{s,d}^0 \rightarrow \ell^+ \ell^-$ Decays in Two-Higgs Doublet Models

Xin-Qiang Li

*Institute of Particle Physics and Key Laboratory of Quark and Lepton Physics (MOE),
Central China Normal University, Wuhan, Hubei 430079, P. R. China*

*State Key Laboratory of Theoretical Physics, Institute of Theoretical Physics,
Chinese Academy of Sciences, Beijing 100190, P. R. China*

Jie Lu¹, Antonio Pich

IFIC, Universitat de València – CSIC, Apt. Correus 22085, E-46071 València, Spain

Abstract

We study the rare leptonic decays $B_{s,d}^0 \rightarrow \ell^+ \ell^-$ within the general framework of the aligned two-Higgs doublet model [1]. A complete one-loop calculation of the relevant short-distance Wilson coefficients is presented, with a detailed technical summary of the results. The phenomenological constraints imposed by present data on the model parameters are also investigated.

Keywords: Rare decays, two-Higgs doublet model, Wilson coefficients, Z_2 symmetry

1. Introduction

The discovery [2, 3] of a Higgs-like boson at the LHC has placed the last missing piece of the Standard Model (SM), which is one of the greatest achievements of modern particle physics. However, it is widely believed that the SM cannot be the fundamental theory up to the Planck scale, and many theories beyond the SM (BSM) claim that new physics (NP) should appear around the TeV scale.

One of the simplest extensions of the SM is the addition of an extra Higgs doublet [4]. Two scalar doublets are present in several BSM theories, for instance in supersymmetry. Two-Higgs doublet models (2HDMs) with generic Yukawa couplings give rise to dangerous tree-level flavour-changing neutral currents (FCNCs) [5]. This can be avoided imposing discrete Z_2 symmetries [6] or, more generally, assuming the alignment in flavour space of the two Yukawa matrices for each type of right-handed fermions [7].

The leptonic decays $B_{s,d}^0 \rightarrow \ell^+ \ell^-$ play a very special role in testing the SM and probing BSM physics. They are very sensitive to the mechanism of quark flavour mixing, and their branching ratios are extremely small due to the loop suppression and the helicity suppression factor m_ℓ/m_b . Since the final state involves only leptons, the SM theoretical predictions are very clean [8]:

$$\overline{\mathcal{B}}(B_s^0 \rightarrow \mu^+ \mu^-) = (3.65 \pm 0.23) \times 10^{-9}, \quad (1)$$

$$\overline{\mathcal{B}}(B_d^0 \rightarrow \mu^+ \mu^-) = (1.06 \pm 0.09) \times 10^{-10}, \quad (2)$$

which include next-to-leading order (NLO) electroweak corrections [9] and next-to-next-to-leading order (NNLO) QCD corrections [10].

The weighted world averages of the CMS [11] and LHCb [12] measurements [13]

$$\overline{\mathcal{B}}(B_s^0 \rightarrow \mu^+ \mu^-)_{\text{exp.}} = (2.9 \pm 0.7) \times 10^{-9}, \quad (3)$$

$$\overline{\mathcal{B}}(B_d^0 \rightarrow \mu^+ \mu^-)_{\text{exp.}} = (3.6_{-1.4}^{+1.6}) \times 10^{-10}, \quad (4)$$

are very close to the SM predictions and put stringent constraints on BSM physics.

¹Speaker

2. The aligned two-Higgs doublet model

It is convenient to define the 2HDM in the ‘‘Higgs basis’’ where only one scalar doublet gets a nonzero vacuum expectation value $v = (\sqrt{2}G_F)^{-1/2} \simeq 246$ GeV:

$$\Phi_1 = \left[\begin{array}{c} G^+ \\ \frac{1}{\sqrt{2}}(v + S_1 + iG^0) \end{array} \right], \quad (5)$$

$$\Phi_2 = \left[\begin{array}{c} H^+ \\ \frac{1}{\sqrt{2}}(S_2 + iS_3) \end{array} \right]. \quad (6)$$

The first doublet contains the Goldstone fields G^\pm and G^0 . The five physical degrees of freedom are given by the two charged fields $H^\pm(x)$ and three neutral scalars $\varphi_i^0(x) = \{h(x), H(x), A(x)\}$. The latter are related with the S_i fields through an orthogonal transformation \mathcal{R} , which defines the neutral mass eigenstates:

$$\mathcal{R} \mathcal{M} \mathcal{R}^T = \text{diag}(M_h^2, M_H^2, M_A^2), \quad \varphi_i^0 = \mathcal{R}_{ij} S_j. \quad (7)$$

The mass matrix \mathcal{M} of the neutral scalars is fixed by the scalar potential:

$$\begin{aligned} V = & \mu_1 (\Phi_1^\dagger \Phi_1) + \mu_2 (\Phi_2^\dagger \Phi_2) + [\mu_3 (\Phi_1^\dagger \Phi_2) + \mu_3^* (\Phi_2^\dagger \Phi_1)] \\ & + \lambda_1 (\Phi_1^\dagger \Phi_1)^2 + \lambda_2 (\Phi_2^\dagger \Phi_2)^2 \\ & + \lambda_3 (\Phi_1^\dagger \Phi_1) (\Phi_2^\dagger \Phi_2) + \lambda_4 (\Phi_1^\dagger \Phi_2) (\Phi_2^\dagger \Phi_1) \quad (8) \\ & + [(\lambda_5 \Phi_1^\dagger \Phi_2 + \lambda_6 \Phi_1^\dagger \Phi_1 + \lambda_7 \Phi_2^\dagger \Phi_2) (\Phi_1^\dagger \Phi_2) + \text{h.c.}], \end{aligned}$$

where μ_1, μ_2 and $\lambda_{1,2,3,4}$ are real, while μ_3 and $\lambda_{5,6,7}$ can be complex.

In the CP-conserving limit, the neutral Higgs spectrum contains a CP-odd field $A = S_3$ and two CP-even scalars h and H which mix through the two-dimensional rotation matrix:

$$\begin{pmatrix} h \\ H \end{pmatrix} = \begin{pmatrix} \cos \tilde{\alpha} & \sin \tilde{\alpha} \\ -\sin \tilde{\alpha} & \cos \tilde{\alpha} \end{pmatrix} \begin{pmatrix} S_1 \\ S_2 \end{pmatrix}. \quad (9)$$

We use the conventions $M_h \leq M_H$, and $0 \leq \tilde{\alpha} \leq \pi$ so that $\sin \tilde{\alpha}$ is always positive.

2.1. Yukawa sector

The 2HDM Yukawa sector is given by

$$\begin{aligned} \mathcal{L}_Y = & -\frac{\sqrt{2}}{v} \left[\bar{Q}'_L (M'_d \Phi_1 + Y'_d \Phi_2) d'_R \right. \\ & + \bar{Q}'_L (M'_u \tilde{\Phi}_1 + Y'_u \tilde{\Phi}_2) u'_R \\ & \left. + \bar{L}'_L (M'_\ell \Phi_1 + Y'_\ell \Phi_2) \ell'_R \right] + \text{h.c.}, \quad (10) \end{aligned}$$

with $\tilde{\Phi}_i(x) = i\tau_2 \Phi_i^*(x)$ the charge-conjugated scalar doublets with hypercharge $Y = -\frac{1}{2}$. Q'_L and L'_L denote

the SM left-handed quark and lepton doublets, respectively, and u'_R, d'_R and ℓ'_R are the corresponding right-handed singlets, in the weak interaction basis.

The Yukawa couplings M'_f and Y'_f ($f = u, d, \ell$) are complex 3×3 matrices which, in general, cannot be diagonalized simultaneously, generating FCNCs at tree level. This can be avoided by assuming that M'_f and Y'_f are proportional to each other [7]. In the mass-eigenstate fermion basis with diagonal matrices M_f , one has then

$$Y_{d,\ell} = \varsigma_{d,\ell} M_{d,\ell}, \quad Y_u = \varsigma_u^* M_u, \quad (11)$$

with arbitrary complex parameters ς_f ($f = d, u, \ell$), which introduce new sources of CP violation. The aligned 2HDM (A2HDM) Yukawa Lagrangian reads

$$\begin{aligned} \mathcal{L}_Y = & -\frac{\sqrt{2}}{v} H^+ \left\{ \bar{u} \left[\varsigma_d V M_d P_R - \varsigma_u M_u^\dagger V P_L \right] d \right. \\ & \left. + \varsigma_\ell \bar{\nu} M_\ell P_R \ell \right\} - \frac{1}{v} \sum_{\varphi_i^0, f} y_f^{\varphi_i^0} \varphi_i^0 \left[\bar{f} M_f P_R f \right] + \text{h.c.}, \quad (12) \end{aligned}$$

where $P_{R,L} \equiv \frac{1 \pm \gamma_5}{2}$, V is the CKM quark-mixing matrix and the neutral Yukawa couplings are given by

$$y_{d,\ell}^{\varphi_i^0} = \mathcal{R}_{i1} + (\mathcal{R}_{i2} + i\mathcal{R}_{i3}) \varsigma_{d,\ell}, \quad (13)$$

$$y_u^{\varphi_i^0} = \mathcal{R}_{i1} + (\mathcal{R}_{i2} - i\mathcal{R}_{i3}) \varsigma_u^*. \quad (14)$$

The usual Z_2 symmetric models can be recovered with specific assignments of the alignment parameters.

2.2. Flavour misalignment

The alignment conditions (11) presumably hold at some high-energy scale Λ_A and are spoiled by radiative corrections which induce a misalignment of the Yukawa matrices. However, the flavour symmetries of the A2HDM tightly constrain the possible FCNC structures, keeping their effects well below the present experimental bounds. The only FCNC local structures induced at one loop take the form [7, 14],

$$\begin{aligned} \mathcal{L}_{\text{FCNC}} = & \frac{C}{4\pi^2 v^3} (1 + \varsigma_u^* \varsigma_d) \\ & \times \sum_i \varphi_i^0 \left\{ (\mathcal{R}_{i2} + i\mathcal{R}_{i3}) (\varsigma_d - \varsigma_u) \left[\bar{d}_L V^\dagger M_u M_u^\dagger V M_d d_R \right] \right. \\ & \left. - (\mathcal{R}_{i2} - i\mathcal{R}_{i3}) (\varsigma_d^* - \varsigma_u^*) \left[\bar{u}_L V M_d M_d^\dagger V^\dagger M_u u_R \right] \right\} + \text{h.c.}. \quad (15) \end{aligned}$$

The renormalization of the misalignment parameter C is determined to be [14]

$$C = C_R(\mu) + \frac{1}{2} \left\{ \frac{2\mu^{D-4}}{D-4} + \gamma_E - \ln(4\pi) \right\}, \quad (16)$$

and absorbs the UV divergences from one-loop Higgs-penguin diagrams in $B_{s,d}^0 \rightarrow \ell^+ \ell^-$ decays [1].

3. Effective Hamiltonian

The low-energy effective Hamiltonian describing $B_{s,d}^0 \rightarrow \ell^+ \ell^-$ decays is given by [15, 16, 17]

$$\mathcal{H}_{\text{eff}} = -\frac{G_F \alpha}{\sqrt{2} \pi s_W^2} \left[V_{tb} V_{tq}^* \sum_i^{10,S,P} C_i \mathcal{O}_i + \text{h.c.} \right],$$

$$\begin{aligned} \mathcal{O}_{10} &= (\bar{q} \gamma_\mu P_L b) (\bar{\ell} \gamma^\mu \gamma_5 \ell), \\ \mathcal{O}_S &= \frac{m_\ell m_b}{M_W^2} (\bar{q} P_R b) (\bar{\ell} \ell), \\ \mathcal{O}_P &= \frac{m_\ell m_b}{M_W^2} (\bar{q} P_R b) (\bar{\ell} \gamma_5 \ell), \end{aligned} \quad (17)$$

where $\ell = e, \mu, \tau$; $q = d, s$, and $m_b = m_b(\mu)$ denotes the b -quark $\overline{\text{MS}}$ running mass. Other possible operators are neglected because their contributions are either zero or proportional to the light-quark mass m_q .

The anomalous dimension of \mathcal{O}_{10} is zero due to the conservation of the $(V - A)$ quark current in the massless quark limit. The operators \mathcal{O}_S and \mathcal{O}_P also have zero anomalous dimensions because the μ dependences of $m_b(\mu)$ and the scalar current $(\bar{q} P_R b)(\mu)$ cancel each other. Therefore the Wilson coefficients C_i do not receive additional renormalization from QCD corrections.

4. Calculation of the Wilson coefficients $C_{10,S,P}$

The Wilson coefficients $C_{10,S,P}$ are obtained by requiring the equality of one-particle irreducible amputated Green functions in the full and in the effective theories. The relevant Feynman diagrams for a given process can be created by the package `FeynArts` [18], with the model files provided by `FeynRules` [19]. The generated decay amplitudes are evaluated either with the help of `FeynCalc` [20], or using standard techniques such as the Feynman parametrization to combine propagators. We found full agreement between the results obtained with these two methods. Throughout the whole calculation, we set the light-quark masses $m_{d,s}$ to zero; while for m_b , we keep it up to linear order.

In general, the Wilson coefficients C_i are functions of the internal up-type quark masses, together with the corresponding CKM factors [21]:

$$C_i = \sum_{j=u,c,t} V_{jq}^* V_{jb} F_i(x_j), \quad (18)$$

where $x_j = m_j^2/M_W^2$, and $F_i(x_j)$ denote the loop functions. In deriving the effective Hamiltonian (17), the limit $m_{u,c} \rightarrow 0$ and the unitarity of the CKM matrix,

$$V_{uq}^* V_{ub} + V_{cq}^* V_{cb} + V_{tq}^* V_{tb} = 0, \quad (19)$$

have to be exploited. This implies that we need only to calculate explicitly the contributions from internal top quarks, while those from up and charm quarks are taken into account by means of simply omitting the mass-independent terms in the basic functions $F_i(x_i)$.

The relevant Feynman diagrams are split into various box, penguin and self-energy diagrams, which are mediated by the top quark, gauge bosons, and Higgs scalars. In order to check the gauge independence of the final results, we perform the calculation both in the Feynman ($\xi = 1$) and in the unitary ($\xi = \infty$) gauges.

4.1. Wilson coefficients in the SM

In the SM, the dominant contribution to the decays $B_{s,d}^0 \rightarrow \ell^+ \ell^-$ comes from the Wilson coefficient C_{10} , which arises from W -box and Z -penguin diagrams:

$$C_{10}^{\text{SM}} = -\eta_Y^{\text{EW}} \eta_Y^{\text{QCD}} Y_0(x_t), \quad (20)$$

where

$$Y_0(x_t) = \frac{x_t}{8} \left[\frac{x_t - 4}{x_t - 1} + \frac{3x_t}{(x_t - 1)^2} \ln x_t \right] \quad (21)$$

is the one-loop Inami-Lim function [22]. The factors η_Y^{EW} and η_Y^{QCD} account for the NLO electroweak [9] and the NNLO QCD corrections [10], respectively.

The coefficients C_S and C_P receive SM contributions from box, Z penguin, Goldstone-boson (GB) penguin and Higgs (h) penguin diagrams:

$$C_S^{\text{SM}} = C_S^{\text{box, SM}} + C_S^{\text{h penguin, SM}}, \quad (22)$$

$$C_P^{\text{SM}} = C_P^{\text{box, SM}} + C_P^{\text{Z penguin, SM}} + C_P^{\text{GB penguin, SM}}. \quad (23)$$

The Goldstone contribution is of course absent in the unitary gauge. Explicit expressions can be found in [1].

4.2. Wilson coefficients in the A2HDM

In the A2HDM there are additional contributions from box and Z penguin diagrams, involving H^\pm exchanges, and from Higgs penguin diagrams. The only new contribution to C_{10} comes from Z penguin diagrams and is gauge independent by itself:

$$C_{10}^{\text{A2HDM}} = C_{10}^{\text{Z penguin, A2HDM}}. \quad (24)$$

The Z penguin diagrams also generate contributions to C_P . The sum of Z penguin diagrams and Goldstone-boson penguin diagrams is gauge independent:

$$C_{P, \text{Unitary}}^{\text{Z penguin, A2HDM}} = C_{P, \text{Feynman}}^{\text{Z penguin, A2HDM}} + C_{P, \text{Feynman}}^{\text{GB penguin, A2HDM}}. \quad (25)$$

The contributions from box diagrams with H^\pm bosons, $C_{S,P}^{\text{box, A2HDM}}$, are gauge dependent.

Neutral scalar exchanges induce both tree and loop diagrams. The loop contributions consist of the Higgs-penguin and self-energy diagrams governed by the Yukawa couplings (12), whereas the tree ones are given by the misalignment couplings (15). The sum of these contributions can be written as:

$$C_S^{\varphi_i^0, \text{A2HDM}} = \sum_{\varphi_i^0} \text{Re}(y_\ell^{\varphi_i^0}) \hat{C}^{\varphi_i^0}, \quad (26)$$

$$C_P^{\varphi_i^0, \text{A2HDM}} = i \sum_{\varphi_i^0} \text{Im}(y_\ell^{\varphi_i^0}) \hat{C}^{\varphi_i^0}, \quad (27)$$

with

$$\begin{aligned} \hat{C}^{\varphi_i^0} = x_t & \left\{ \frac{(S_u - S_d)(1 + S_u^* S_d)}{2x_{\varphi_i^0}} (\mathcal{R}_{i2} + i\mathcal{R}_{i3}) C_R(M_W) \right. \\ & \left. + \frac{v^2}{M_{\varphi_i^0}^2} \lambda_{H^+ H^-}^{\varphi_i^0} g_0 + \sum_{j=1}^3 \mathcal{R}_{ij} \xi_j \left[\frac{g_j^{(a)}}{2x_{\varphi_i^0}} + g_j^{(b)} \right] \right\}, \quad (28) \end{aligned}$$

where $\lambda_{H^+ H^-}^{\varphi_i^0} = \lambda_3 \mathcal{R}_{i1} + \lambda_7^R \mathcal{R}_{i2} - \lambda_7^I \mathcal{R}_{i3}$, $\xi_1 = \xi_2 = 1$ and $\xi_3 = i$. When $\zeta_{u,d} \rightarrow 0$, $x_{H,A} \rightarrow \infty$, $x_h \rightarrow x_{h_{\text{SM}}}$, $\mathcal{R}_{i2,i3} \rightarrow 0$ and $\mathcal{R}_{i1} \rightarrow 1$, this reproduces the SM result.

The coefficients g_0 , $g_j^{(a)}$ and $g_j^{(b)}$ are functions of x_t , x_{H^+} , ζ_u and ζ_d . g_0 and $g_j^{(a)}$ are gauge independent because they do not involve any gauge bosons, while $g_j^{(b)}$ are all related to Goldstone-boson vertices and, therefore, are identically zero in the unitary gauge. These $g_j^{(b)}$ contributions cancel the gauge dependence from the box diagrams:

$$C_{S, \text{Unitary}}^{\text{box, SM}} - C_{S, \text{Feynman}}^{\text{box, SM}} = x_t g_1^{(b)}, \quad (29)$$

$$C_{S, \text{Unitary}}^{\text{box, A2HDM}} - C_{S, \text{Feynman}}^{\text{box, A2HDM}} = x_t \left[\text{Re}(\zeta_\ell) g_2^{(b)} - i \text{Im}(\zeta_\ell) g_3^{(b)} \right], \quad (30)$$

$$C_{P, \text{Unitary}}^{\text{box, A2HDM}} - C_{P, \text{Feynman}}^{\text{box, A2HDM}} = x_t \left[i \text{Im}(\zeta_\ell) g_2^{(b)} - \text{Re}(\zeta_\ell) g_3^{(b)} \right]. \quad (31)$$

The loop contributions with neutral scalar exchanges generate UV divergences which are cancelled by the renormalization of the misalignment coupling in (16). The μ dependence of the results is reabsorbed into the combination $C_R(M_W) = C_R(\mu) - \ln(M_W/\mu)$.

5. Phenomenological analysis

Currently, only $B_s \rightarrow \mu^+ \mu^-$ is observed with a signal significance of $\sim 4.0 \sigma$ [13]. Thus we shall investigate the allowed parameter space of the A2HDM under the

constraint from $\overline{\mathcal{B}}(B_s^0 \rightarrow \mu^+ \mu^-)$. With updated input parameters, the SM prediction reads

$$\overline{\mathcal{B}}(B_s^0 \rightarrow \mu^+ \mu^-)_{\text{SM}} = (3.67 \pm 0.25) \times 10^{-9}. \quad (32)$$

In order to explore constraints on the model parameters, it is convenient to introduce the ratio [15, 16]

$$\overline{R}_{s\ell} \equiv \frac{\overline{\mathcal{B}}(B_s^0 \rightarrow \ell^+ \ell^-)}{\overline{\mathcal{B}}(B_s^0 \rightarrow \ell^+ \ell^-)_{\text{SM}}} = \left[|P|^2 + \left(1 - \frac{\Delta\Gamma_s}{\Gamma_L^s}\right) |S|^2 \right], \quad (33)$$

where $\Gamma_{L(H)}^s$ denote the lighter (heavier) eigenstate decay width of the B_s meson, and $\Delta\Gamma_s = \Gamma_L^s - \Gamma_H^s$. The quantities S and P are defined as

$$P \equiv \frac{C_{10}}{C_{10}^{\text{SM}}} + \frac{M_{B_s}^2}{2M_W^2} \left(\frac{m_b}{m_b + m_s} \right) \frac{C_P - C_P^{\text{SM}}}{C_{10}^{\text{SM}}}, \quad (34)$$

$$S \equiv \sqrt{1 - \frac{4m_\ell^2}{M_{B_s}^2}} \frac{M_{B_s}^2}{2M_W^2} \left(\frac{m_b}{m_b + m_s} \right) \frac{C_S - C_S^{\text{SM}}}{C_{10}^{\text{SM}}}, \quad (35)$$

where the Wilson coefficients are given by:

$$C_{10} = C_{10}^{\text{SM}} + C_{10}^{\text{Z penguin, A2HDM}},$$

$$C_S = C_S^{\text{box, SM}} + C_S^{\text{box, A2HDM}} + C_S^{\varphi_i^0, \text{A2HDM}},$$

$$C_P = C_P^{\text{SM}} + C_P^{\text{box, A2HDM}} + C_P^{\varphi_i^0, \text{A2HDM}} + C_P^{\text{Z penguin, A2HDM}} + C_P^{\text{GB penguin, A2HDM}}. \quad (36)$$

Combining the SM prediction (32) with the latest experimental result (3), we get

$$\overline{R}_{s\mu} = 0.79 \pm 0.20. \quad (37)$$

5.1. Model parameters

We consider the CP-conserving limit and assume that the lightest CP-even scalar h corresponds to the observed neutral boson with $M_h \simeq 126$ GeV. We have then 10 free parameters: 3 alignment couplings ζ_f , 3 scalar masses (M_H, M_A, M_{H^\pm}), 2 scalar-potential couplings (λ_3, λ_7), the mixing angle $\tilde{\alpha}$ and the misalignment parameter $C_R(M_W)$. Four of them ($\tilde{\alpha}, \lambda_{3,7}, C_R(M_W)$) have minor impacts on $\overline{R}_{s\mu}$, compared to the others. In order to simplify the analysis, we assign them the following values, using the bounds from earlier studies:

$$\lambda_3 = \lambda_7 = 1, \quad \cos \tilde{\alpha} = 0.95, \quad C_R(M_W) = 0. \quad (38)$$

The $C_{S,P}$ contributions to (34) and (35) are suppressed by a factor $M_{B_s}^2/M_W^2$. Therefore, unless there are large enhancements from the ζ_f parameters, the branching ratio shall be dominated by C_{10} , where the A2HDM

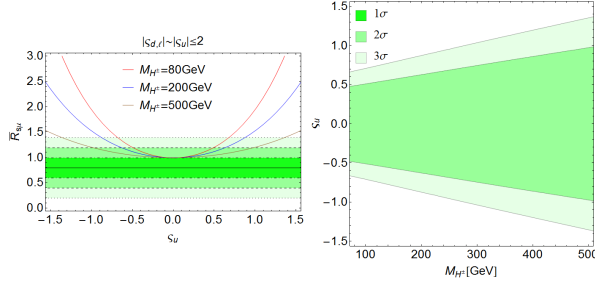


Figure 1: Dependence of \bar{R}_{su} on ζ_u (left) and resulting upper bounds on ζ_u (right), as function of M_{H^\pm} , for $|\zeta_{d,\ell}| \lesssim |\zeta_u| \le 2$.

contribution depends only on $|\zeta_u|^2$ and M_{H^\pm} . We shall then discuss two possible scenarios: 1) $|\zeta_{d,\ell}| \lesssim |\zeta_u| \le 2$, where C_{10} dominates, and 2) $|\zeta_{d,\ell}| \gg |\zeta_u|$, where C_S and C_P could play a significant role.

5.2. Small $\zeta_{d,\ell}$

The only relevant NP contribution is C_{10}^{A2HDM} which involves two parameters, ζ_u and M_{H^\pm} . The constraints imposed by \bar{R}_{su} are shown in Fig. 1. In the left panel, we choose $M_{H^\pm} = 80, 200$ and 500 GeV (upper, middle and lower curves, respectively). The shaded horizontal bands denote the allowed experimental region at 1σ (dark green), 2σ (green), and 3σ (light green), respectively. The right panel shows the resulting upper bounds on ζ_u , as function of M_{H^\pm} . A 95% CL upper bound $|\zeta_u| \le 0.49$ (0.97) is obtained for $M_{H^\pm} = 80$ (500) GeV. Since $C_{10}^{A2HDM} \sim |\zeta_u|^2$, this constraint is independent of any assumption about CP. For larger masses the constraint becomes weaker since the H^\pm contribution starts to decouple.

5.3. Large $\zeta_{d,\ell}$

In this case, C_S and C_P can induce a significant impact on the branching ratio. We vary ζ_d and ζ_ℓ within the range $[-50, 50]$, and choose three representative values for $\zeta_u = 0, \pm 1$. We also take three different representative sets of scalar masses:

$$\begin{aligned} \text{Mass1 : } & M_{H^\pm} = M_A = 80 \text{ GeV}, \quad M_H = 130 \text{ GeV}, \\ \text{Mass2 : } & M_{H^\pm} = M_A = M_H = 200 \text{ GeV}, \\ \text{Mass3 : } & M_{H^\pm} = M_A = M_H = 500 \text{ GeV}. \end{aligned} \quad (39)$$

In Fig. 2, we show the allowed regions in the ζ_d - ζ_ℓ plane under the constraint from \bar{R}_{su} . The regions with large ζ_d and ζ_ℓ are already excluded, especially when they have the same sign. The impact of ζ_u is significant: a nonzero ζ_u will exclude most of the regions allowed in the case with $\zeta_u = 0$, and changing the sign of ζ_u

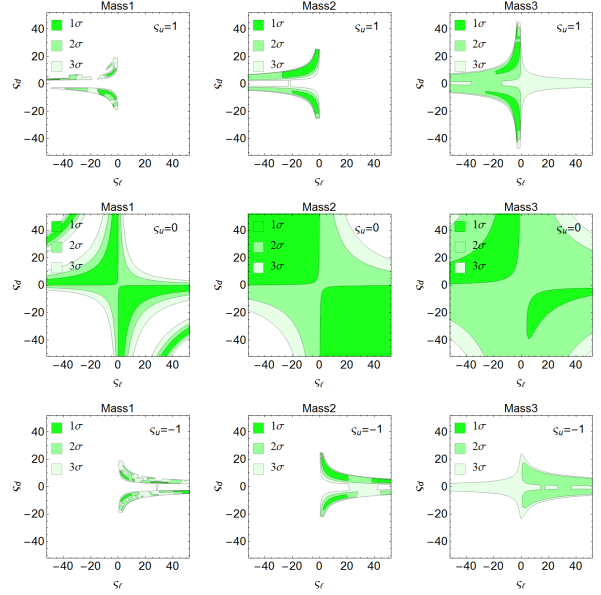


Figure 2: Allowed regions (at 1σ , 2σ and 3σ) in the ζ_d - ζ_ℓ plane under the constraint from \bar{R}_{su} , with three different assignments of the scalar masses and $\zeta_u = 0, \pm 1$.

Model	S_d	S_u	S_ℓ
Type I	$\cot\beta$	$\cot\beta$	$\cot\beta$
Type II	$-\tan\beta$	$\cot\beta$	$-\tan\beta$
Type X (lepton-specific)	$\cot\beta$	$\cot\beta$	$-\tan\beta$
Type Y (flipped)	$-\tan\beta$	$\cot\beta$	$\cot\beta$
Inert	0	0	0

Table 1: 2HDMs based on discrete Z_2 symmetries.

will also flip that of ζ_ℓ . The allowed regions expand with increasing scalar masses, as expected, since the NP contributions gradually decouple from the SM.

5.4. 2HDMs with discrete Z_2 symmetries

The usual Z_2 symmetric models are recovered for the values of ζ_f indicated in Table 1. In these models, the ratio \bar{R}_{su} only involves seven free parameters: M_{H^\pm} , M_H , M_A , λ_3 , λ_7 , $\cos\tilde{\alpha}$ and $\tan\beta$. In the particular case of the type-II 2HDM at large $\tan\beta$, our results agree with the ones calculated in Ref. [23]. It is also interesting to note that the $B_{S,d}^0 \rightarrow \ell^+\ell^-$ branching ratios depend only on the charged-Higgs mass and $\tan\beta$ in this case.

Fig. 3 shows the dependence of \bar{R}_{su} on $\tan\beta$, for three representative charged-Higgs masses: $M_{H^\pm} = 80, 200$ and 500 GeV. The other two neutral scalar masses have been fixed at $M_H = M_A = 500$ GeV. The four different panels correspond to the models of types I, II, X and Y, respectively. A lower bound $\tan\beta > 1.6$ is obtained

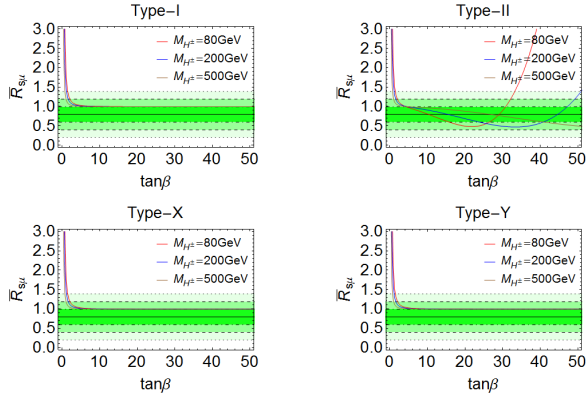


Figure 3: Dependence of \bar{R}_{SM} on $\tan\beta$ for the 2HDMs of types I, II, X and Y. The upper, middle and lower curves correspond to $M_{H^\pm} = 80, 200$ and 500 GeV, respectively. The horizontal bands denote the allowed experimental region at 1σ (dark green), 2σ (green), and 3σ (light green).

at 95% CL under the constraint from the current experimental data on \bar{R}_{SM} . This implies $\zeta_\mu = \cot\beta < 0.63$, which is stronger than the bounds obtained previously from other sources [14, 24].

6. Conclusions

We have studied the rare decays $B_{s,d}^0 \rightarrow \ell^+ \ell^-$ within the general framework of the A2HDM. A complete one-loop calculation of the Wilson coefficients C_{10} , C_5 and C_P has been performed. They arise from various box, penguin and self-energy diagrams, as well as tree-level FCNC diagrams induced by the flavour misalignment interaction (15). The gauge independence of the results has been checked through separate calculations in the Feynman and unitary gauges, and the gauge relations among different diagrams have been examined in detail.

We have also investigated the impact of the current $\bar{\mathcal{B}}(B_s^0 \rightarrow \mu^+ \mu^-)$ data on the model parameters, especially the resulting constraints on the three alignment couplings ζ_f . This information is complementary to the one obtained from collider physics and will be useful for future global data fits within the A2HDM.

Acknowledgements

Work supported by the NSFC [contracts 11005032 and 11435003], the Spanish Government [FPA2011-23778] and Generalitat Valenciana [PROMETEOII/2013/007]. X. Li was also supported by the Scientific Research Foundation for the Returned Overseas Chinese Scholars, State Education Ministry.

J. Lu is grateful for the hospitality of Center for Future High Energy Physics in Beijing.

References

- [1] X. Q. Li, J. Lu and A. Pich, JHEP **1406** (2014) 022 [arXiv:1404.5865 [hep-ph]].
- [2] G. Aad *et al.* [ATLAS Collaboration], Phys. Lett. B **716** (2012) 1 [arXiv:1207.7214 [hep-ex]].
- [3] S. Chatrchyan *et al.* [CMS Collaboration], Phys. Lett. B **716** (2012) 30 [arXiv:1207.7235 [hep-ex]].
- [4] T. D. Lee, Phys. Rev. D **8** (1973) 1226.
- [5] G. C. Branco, P. M. Ferreira, L. Lavoura, M. N. Rebelo, M. Sher and J. P. Silva, Phys. Rept. **516** (2012) 1 [arXiv:1106.0034 [hep-ph]]; J. F. Gunion, H. E. Haber, G. L. Kane and S. Dawson, Front. Phys. **80** (2000) 1.
- [6] S. L. Glashow and S. Weinberg, Phys. Rev. D **15** (1977) 1958.
- [7] A. Pich and P. Tuzón, Phys. Rev. D **80** (2009) 091702 [arXiv:0908.1554 [hep-ph]].
- [8] C. Bobeth, M. Gorbahn, T. Hermann, M. Misiak, E. Stamou and M. Steinhauser, Phys. Rev. Lett. **112** (2014) 101801 [arXiv:1311.0903 [hep-ph]].
- [9] C. Bobeth, M. Gorbahn and E. Stamou, Phys. Rev. D **89** (2014) 034023 [arXiv:1311.1348 [hep-ph]].
- [10] T. Hermann, M. Misiak and M. Steinhauser, JHEP **1312** (2013) 097 [arXiv:1311.1347 [hep-ph]].
- [11] S. Chatrchyan *et al.* [CMS Collaboration], Phys. Rev. Lett. **111** (2013) 101804 [arXiv:1307.5025 [hep-ex]].
- [12] R. Aaij *et al.* [LHCb Collaboration], Phys. Rev. Lett. **111** (2013) 101805 [arXiv:1307.5024 [hep-ex]].
- [13] CMS and LHCb Collaborations [CMS and LHCb Collaboration], CMS-PAS-BPH-13-007.
- [14] M. Jung, A. Pich and P. Tuzón, JHEP **1011** (2010) 003 [arXiv:1006.0470 [hep-ph]].
- [15] A. J. Buras, R. Fleischer, J. Girrbach and R. Knegjens, JHEP **1307** (2013) 77 [arXiv:1303.3820 [hep-ph]].
- [16] K. De Bruyn, R. Fleischer, R. Knegjens, P. Koppenburg, M. Merk, A. Pellegrino and N. Tuning, Phys. Rev. Lett. **109** (2012) 041801 [arXiv:1204.1737 [hep-ph]].
- [17] W. Altmannshofer, P. Paradisi and D. M. Straub, JHEP **1204** (2012) 008 [arXiv:1111.1257 [hep-ph]].
- [18] T. Hahn, Comput. Phys. Commun. **140** (2001) 418 [hep-ph/0012260].
- [19] N. D. Christensen and C. Duhr, Comput. Phys. Commun. **180** (2009) 1614 [arXiv:0806.4194 [hep-ph]]; A. Alloul, N. D. Christensen, C. Degrande, C. Duhr and B. Fuks, arXiv:1310.1921 [hep-ph].
- [20] R. Mertig, M. Bohm and A. Denner, Comput. Phys. Commun. **64** (1991) 345.
- [21] G. Buchalla, A. J. Buras and M. E. Lautenbacher, Rev. Mod. Phys. **68** (1996) 1125 [hep-ph/9512380]; A. J. Buras, hep-ph/9806471.
- [22] T. Inami and C. S. Lim, Prog. Theor. Phys. **65** (1981) 297 [Erratum-ibid. **65** (1981) 1772].
- [23] H. E. Logan and U. Nierste, Nucl. Phys. B **586** (2000) 39 [hep-ph/0004139].
- [24] M. Jung, A. Pich and P. Tuzón, Phys. Rev. D **83** (2011) 074011 [arXiv:1011.5154 [hep-ph]]; M. Jung, X.-Q. Li and A. Pich, JHEP **1210** (2012) 063 [arXiv:1208.1251 [hep-ph]]; A. Celis, M. Jung, X.-Q. Li and A. Pich, JHEP **1301** (2013) 054 [arXiv:1210.8443 [hep-ph]]; L. Duarte, G. A. González-Sprinberg and J. Vidal, JHEP **1311** (2013) 114 [arXiv:1308.3652 [hep-ph]]; M. Jung and A. Pich, JHEP **1404** (2014) 076 [arXiv:1308.6283 [hep-ph]].